

Effect of vimentin on cell migration in collagen-coated microchannels: A mimetic physiological confined environment

Cite as: Biomicrofluidics 15, 034105 (2021); doi: 10.1063/5.0045197

Submitted: 24 January 2021 · Accepted: 2 May 2021 ·

Published Online: 18 May 2021



View Online



Export Citation



CrossMark

Zhiru Zhou,¹ Feiyun Cui,¹ Qi Wen,² and H. Susan Zhou^{1,a)}

AFFILIATIONS

¹ Department of Chemical Engineering, Worcester Polytechnic Institute, 100 Institute Road, Worcester, Massachusetts 01609, USA

² Department of Physics, Worcester Polytechnic Institute, Worcester, Massachusetts 01609, USA

^{a)}Author to whom correspondence should be addressed: szhou@wpi.edu

ABSTRACT

Cancer cell migration through tissue pores and tracks into the bloodstream is a critical biological step for cancer metastasis. Although *in vivo* studies have shown that expression of vimentin can induce invasive cell lines, its role in cell cytoskeleton reorganization and cell motility under *in vitro* physical confinement remains unknown. Here, a microfluidic device with cell culture chamber and collagen-coated microchannels was developed as an *in vitro* model for physiological confinement environments. Using this microchannel assay, we demonstrated that the knockdown of vimentin decreases 3T3 fibroblast cell directional migration speed in confined microchannels. Additionally, as cells form dynamic membranes that define the leading edge of motile cells, different leading edge morphologies of 3T3 fibroblast and 3T3 vimentin knockdown cells were observed. The leading edge morphology change under confinement can be explained by the effect of vimentin on cytoskeletal organization and focal adhesion. The microfluidic device integrated with a time-lapse microscope provided a new approach to study the effect of vimentin on cell adhesion, migration, and invasiveness.

Published under an exclusive license by AIP Publishing. <https://doi.org/10.1063/5.0045197>

INTRODUCTION

Cell migration and motility are important for many physiological and pathological processes, such as wound healing^{1,2} and cancer metastasis.^{3,4} The extracellular matrix (ECM) is an important component in providing mechanical support for tissues and cells, generating cell signals that are capable of affecting cell adhesion and migration, and establishing the cellular environment.⁵ Cells migrating *in vivo* experience varying degree of confinement as the ECM microenvironment offers many tracks for cell migration, including tracks along ECM fibers or blood vessels, between connective tissue and the basement membrane of muscle, in the interstitial space, or in the vasculature of organs.⁶ The simplicity of the 2D flat surface showed limitation to mimic the track and does not faithfully capture the physiological behavior of cell migration *in vivo*. Thus, a 3D microchannel will elicit a more complicated environment with physiological cues containing mechanical cues,⁷ adhesive cues,⁸ ECM-bound cues,⁹ and topographical cues.¹⁰ Many bioengineering models have been built for the study of cell migration, such as polydimethylsiloxane (PDMS) microfluidic devices,¹¹

3D hydrogels,¹² and microcontact printed islands.¹³ The PDMS microfluidic device currently has the most potential as it is capable of providing precise control¹⁴ of mechanical, physical, chemical, and topographic cues.

The cell cytoskeleton is a group of dynamic proteins that are important for increasing cell adhesion, regulating cell shape and motility, and maintaining cell integrity. The cell cytoskeleton is composed of microtubules, actin filaments, and intermediate filaments. Vimentin is a component of type III intermediate filament protein existing in motile mesenchymal cells, including fibroblasts, macrophages,¹⁵ and metastasis cancer cells. There is evidence that vimentin is involved in the regulation of cell morphology, adhesion, and motility. Overexpression of vimentin is observed in various types of cancers including prostate cancer, lung cancer, malignant melanoma, and breast cancer, which links overexpression of vimentin to the invasiveness of cancer.¹⁶ This correlation can be explained, as vimentin is a marker for the epithelial-to-mesenchymal transition (EMT) process,¹⁷ a process that occurs during cancer metastasis. Vimentin expression is also correlated with the wound healing process.

Vimentin-knockout mice are defective in the directional migration of fibroblasts and capacity of wound healing.^{18,19} Fibroblasts from the embryos of these mice are incapable of translocation, and the reintroduction of vimentin rescues the motility of these cells. Vimentin knockdown (VimKD) was shown to attenuate the migration of fibroblasts²⁰ and cancer cells.^{21,22} Mendez *et al.*²³ showed in a 2D experiment that expression of vimentin can induce cells to adopt a mesenchymal shape and increase motility. The roles of vimentin in cytoskeleton organization, cell morphology, and motility on flat 2D substrates have been studied extensively.^{23–25} However, fibroblasts often migrate *in vivo* in an extracellular matrix that is intrinsically 3D; hence, the role of vimentin in 3D setting is less well understood.

To address how vimentin regulates cell migration in a 3D setting, a microfluidic device with constriction microchannels coated with collagen type I was designed and developed. Previous investigations reported that collagen promotes 3T3 fibroblast cell migration accompanying the production of matrix metalloproteinases (MMPs) and Reactive oxygen species (ROS).²⁶ Collagen I was shown to be able to initiate human dermal fibroblast migration without growth factors.²⁷ Thus, we assume that a collagen-coated PDMS surface may serve as a good substrate to study cell migration.

Protrusions of 3T3 and 3T3 vimentin knockdown cells (3T3 vim-) cells inside channel were also observed and studied. Protrusions of cell front are highly dynamic structures that provide sustained forward force for cell migration.²⁸ Migrating cells extend different types of plasma membrane protrusions²⁹ including lamellipodia, filopodia, blebs, and invadopodia. Actin cytoskeleton and regulators activated by signaling pathways allow cells to respond dynamically to ECM environments. The mode of cell migration can be classified by the morphology of leading edge and types of structure forming the leading edge.^{30,31} There is a wide diversity in the types of protrusions, while the type of protrusion can be used to define a specific mode of cell migration.

The microfluidic device was then integrated with a cell culture chamber on a microscope, which assures that the 3T3 fibroblast cells and 3T3 vimentin- cells can be cultured and imaged inside the microfluidic device for up to 12 h. High-resolution, real-time images were captured for cell migration inside collagen-coated microchannel. Cell morphology changes and membrane fluctuations were observed under the microscope, which can provide insight into the mechanisms of the cell migration process.

EXPERIMENTAL SECTION

Materials and chemicals

Cell culture

3T3 fibroblasts were bought from NIH. Vimentin knockdown (VimKD) 3T3 line was obtained by transfecting the NIH-3T3 fibroblasts using a lentiviral vector containing short hairpin RNA (shRNA) against mouse vimentin. NIH-3T3 fibroblasts and 3T3 vimentin knockdown (3T3 vim-) cells were maintained in DMEM (Dulbecco's Modified Eagle Medium) (BioWhittaker, Walkersville, MD) supplemented with 10% bovine calf serum (Gibco, Waltham, MA), 2 mM L-glutamine (Gibco), 100 µg/ml streptomycin, and 100 units/ml penicillin (Gibco).

Microfluidic device fabrication and operation

PDMS microchannels were fabricated using standard photolithography and soft lithography processes. The microchannel design was first drawn by AutoCAD and then the pattern was transferred to a chrome-on-glass photolithography mask (Advance Reproductions Corp). To prepare masters, SU-8 2010 and SU-8 2100 epoxy-negative photoresists (Microchem Corp.) were applied by spin coating (Laurell Technologies Corp.) onto silicon wafers in two steps. The first layer of SU-8 2010 was spread at 3500 rpm for 30 s with an acceleration of 300 rpm/s to a final thickness of 10 µm. The SU-8 2010 photoresist was prebaked at 95 °C for 2 min, exposed to 145 mJ/cm² UV radiation through a chrome mask for 7 s, post-baked at 95 °C for 4.5 min, and subsequently developed using SU-8 developer for about 3 min. The silicon wafer was then dried with the first layer pattern using pressurized inert gas. The second layer of SU-8 2100 was then spread onto the wafer at 2200 rpm for 30 s with an acceleration of 300 rpm/s. The wafer was prebaked at 65 °C for 5 min and 95 °C for 15 min. After exposure, the wafer was post-baked at 65 °C for 4 min and 95 °C for 10 min, and subsequently developed with an SU-8 developer for 9 min. After completing the aforementioned steps, the silicon wafer photomask was fabricated and was ready to be used for the following PDMS soft lithography.

A PDMS solution mixer was obtained by mixing prepolymer (Sylgard 184) with cross-linker (Dow Corning) in a 10:1 ratio (by weight) and then poured onto the as-fabricated silicon wafer. After degassing in a vacuum for 1 h, it was incubated at 80 °C for 1 h. After the curing process, the PDMS device can be peeled off the silicon wafer and bonded to a glass slide using oxygen plasma.

Immediately after the oxygen plasma treatment, the device was flushed with a solution of 70% (vol/vol) ethanol in de-ionized water (diH₂O) followed by rinsing with sterile diH₂O for sterilization. Channels were then rinsed with phosphate buffered saline (PBS) and coated with surface ligands by pumping in a 10 µg/ml solution of collagen I (BD Biosciences, Franklin Lakes, NJ) in PBS and incubating for 1 h at 37 °C. Channels were then washed 3× with PBS, filled with cell culture media, and incubated at 37 °C for at least 30 min before seeding cells.

Cell culture and seeding into the microfluidic device

Cells were incubated at 37 °C in a standard 5% CO₂ cell incubator with a humidified atmosphere of 95% air. All experiments were carried out while the cells were in the exponential growth phase. Cells were trypsinized using 0.25% trypsin (Gibco) at 37 °C, then centrifuged to remove the trypsin, and resuspended in cell media at densities of 1 × 10⁶ cells ml⁻¹. Then, the cell-culture media mixture was infused into cell culture chambers with a pipet to allow them to flow into each chamber. Cells were preferentially placed near the opening of the channel constrictions by manually tilting the device for 2–4 min and allowing gravity to pull cells in suspension toward the constrictions. The device was kept in an Imaging Chamber maintained at 37 °C and 5% CO₂. Time-lapse imaging was performed with an IX3 Olympus microscope (Olympus, PA) equipped with a QIClick CCD camera (QImaging, BC, Canada), using SlideBook software (Intelligent Imaging Innovations, CO).

Cell fluorescence fixing and staining inside microfluidic channel

Cells were allowed to protrude into the microchannel before fixing and staining. To fix cells, slowly pipet in 4% paraformaldehyde solution (AMRESCO) and incubate at room temperature for 10 min. Wash the cells with PBS for three times. To stain cell nucleus, slowly pipet in 300 nM DAPI solution (Biotium, Fremont, CA, USA) and incubate at room temperature for 15 min without exposure to light and then wash the cells with PBS three times. To stain cell actin filaments, slowly pipet in Alexa fluor 488 phalloidin solution (Molecular Probes, Eugene, OR, USA) and incubate at room temperature for 5 min without exposure to light and then wash the cells with PBS for three times. The stained cells were then observed under a microscope with L200 mercury and a halogen fluorescent lamp (Prior Scientific, MA).

Cell motility measurements

Cell trajectories were determined by tracking the center of mass of cells at 10 min increments using ImageJ software (NIH) and the Manual Tracking plugin (<https://imagej.nih.gov/ij/>). Cell speed was determined over time t as $v(t) = [r(t + \Delta t) - r(t)] / \Delta t$.

RESULTS AND DISCUSSION

Fabrication and characterization of microfluidic channels

The microfluidic device was fabricated by standard photolithography and soft-lithography processes. The 10 μm height migration microchannels were connected by two 100 μm height cell culture chambers [Fig. 1(a)]. To achieve the height difference, two types of SU-8 were used: SU-8 2010 and SU-8 2100. The images of microchannels were captured by a 20 \times microscope [Fig. 1(b)], which confirmed the channel widths of 5 and 10 μm and channel length of 50 μm .

Molecule scale adhesive cues for cell directional migration

One major problem for cell cultures in PDMS microfluidic devices is cell detachment from the PDMS surface, where cells grew poorly on the native PDMS surface. Surface modifications by ECM proteins such as fibronectin³² and collagen³³ have shown to significantly increase cell viability.

In our experiment, 3T3 fibroblast cells were seeded on the PDMS surface and collagen type I monolayer coated PDMS surface, while cell passage through microchannels was recorded by time-lapse imaging (Fig. 2). Collagen type I, as one of the ECM protein, was shown to promote the adhesion, survival, and proliferation of many cell types such as mesenchymal stem cells³⁴ and endothelial cells.³⁵ To determine if collagen coating influences cell persistent and directional movement, we compared the cell passage rate (numbers of cells crossed channel/numbers of cells entered channel) between two types of 3D matrix microchannels. As is shown in Fig. 2, after collagen coating, both 3T3 fibroblast and 3T3 vim- cells showed a significant increase in the percentage of cells that passed through the channel. After collagen coating, the rate of

cells moving backward inside the channel largely decreased and thus the rate of cell passage increased. The results indicate that in the 3D matrix, a monolayer of collagen can significantly promote cell directional migration inside the channel.

The expression of vimentin knockdown impairs cell migration

Although it is well acknowledged that vimentin knockdown or knockout attenuates the migration of fibroblasts² and that motile and invasive cell lines express higher levels of vimentin, it has not yet been demonstrated in a 3D *in vitro* environment. To test the hypothesis, we designed microchannels with different channel widths (5 and 10 μm) under a confinement height of 10 μm . 3T3 fibroblast and 3T3 vim- cells were seeded on the collagen I-coated microfluidic device in the cell chamber and then spontaneously entered into the channel without any constant chemical gradient. Cell motion was tracked by time-lapse imaging over 12 h. Figure 3(a) shows the whole process of a cell entering into and exiting out of the channel. Cells enter into microchannel by protruding its leading edge and making contact with the channel wall, followed by squeezing and moving forward inside the channel.

The migration velocities of 3T3 fibroblast and 3T3 vim- cells were then compared. As shown in Fig. 3(b), the speed of 3T3 fibroblast cells is much faster than 3T3 vim- fibroblast cells. This result demonstrates that the expression of vimentin knockdown would impair fibroblast cell migration, which explains why vimentin knockdown mice showed impaired wound healing abilities.

The effect of channel width on cell migration velocity was also shown in Fig. 3(b). Both 3T3 and 3T3 vim- cells showed higher migration velocity in the 5 μm width channel compared to the 10 μm width channel. Decreasing channel width will increase the confinement level on the cell inside channel; moderate confinement of cells with length scales greater than the size of nucleus is shown to increase the cell speed.³⁶ A microchannel based device for study of MDA-MB-231 cancer cell migration showed that cells exhibited higher migration velocity in a narrower channel.³⁷ Cells are more “committed” to move through narrower channels than wider channels.

Cell leading edge protrusions during migration

There is great diversity in the types of protrusions where the type of protrusion can be used to define a specific mode of cell migration. Lamellipodia-based migration is characterized by thin veil-like actin-rich extensions at the leading edge. Lamellipodia-based 3D cell migration was found in cancer cells and primary fibroblast cells. A study carried out in a 3D collagen matrix identified that human foreskin fibroblasts use lamellipodia migration in non-linear elasticity and can switch to lobopodian-based migration in linear elasticity.³⁸ This reveals that the modes of 3D cell migration can be governed by the 3D extracellular matrix. Another study was performed on migrating 3T3 fibroblasts constrained to a specific area using micropatterned polyelectrolyte self-assembly.³⁹ Cell migration in confined channels are regulated by cytoskeleton organization. Cells are fixed and stained when their cell leading edge is inside the channel. It is generally accepted that the propulsive actions of the cell body moving forward are dynamic traction

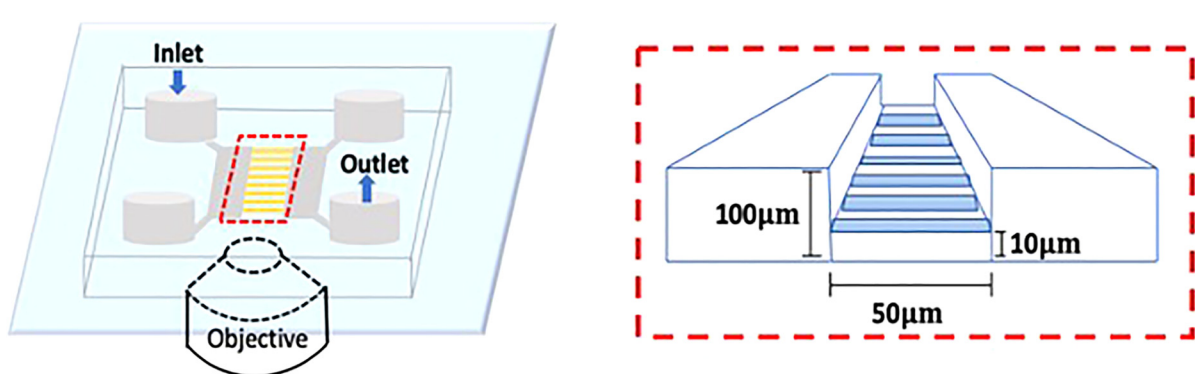
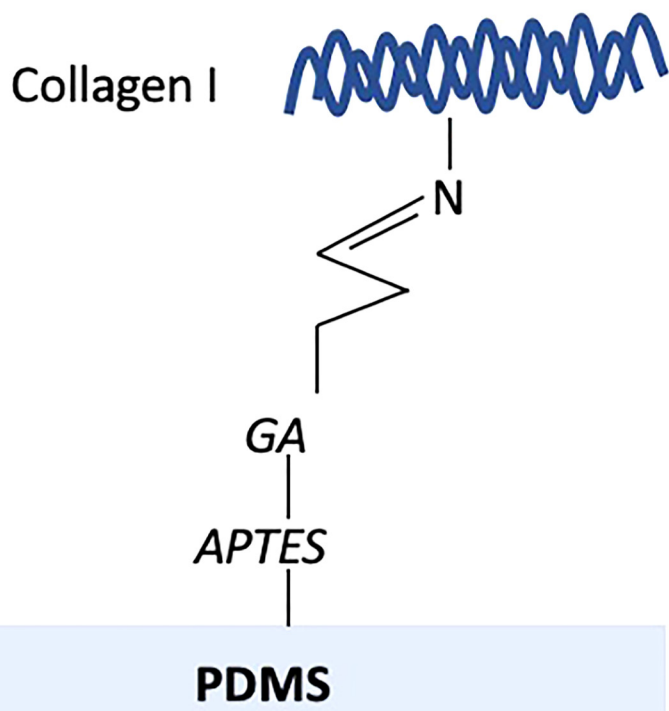
A**B****C**

FIG. 1. (a) schematics of microfluidic device, (b) microscope images of microchannels, and (c) schematic diagram of collagen immobilization on PDMS surface.

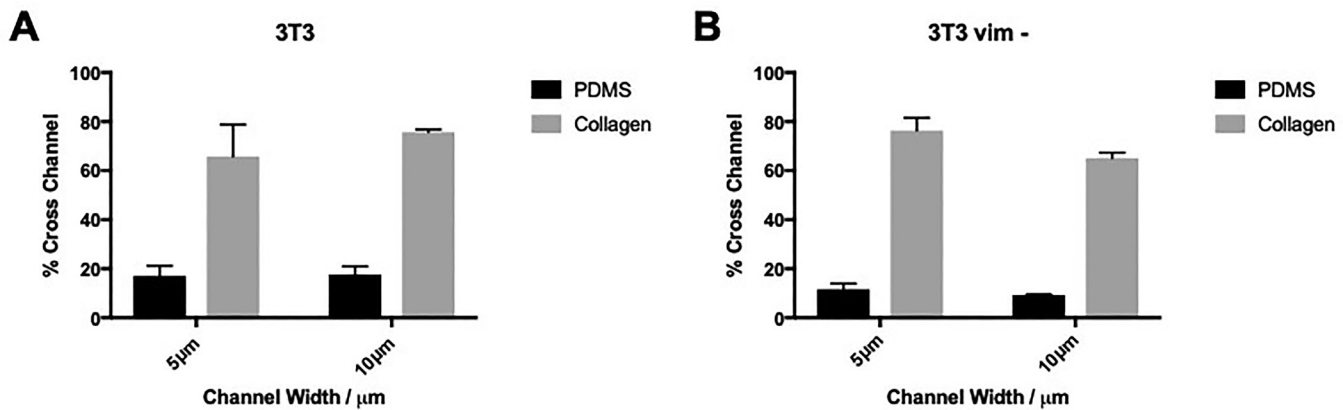


FIG. 2. Effect of surface collagen I coating on cell persistent migration before and after monolayer coating of collagen. (a) Percentage of 3T3 fibroblast cells that crossed 5 and 10 μm width channel. (b) Percentage of 3T3 vim- fibroblast cells that crossed 5 and 10 μm width channel (45–60 cells per condition, N = 3+ experiments).

forces at the leading edge.⁴⁰ Analysis of traction force in polarized migrating 3T3 fibroblast cells indicated that strong inward tractions were localized at the leading edge, lateral protrusion, and sometimes at the trailing edge of the cell.⁴¹ Many *in vitro* studies performed on 2D surfaces^{42,43} have demonstrated that cells migrate by generating lamellipodial protrusions. The protrusions are caused by actin polymerization coupled with cell–matrix adhesion. Similarly, the degree of adhesion and RhoA signaling can uniquely

identify the mode of 3D migration⁴⁴, which can be classified by different types of leading edge protrusions.

In our experiments, cells were fixed and stained after entry into the channel. Actin was stained as red and the nucleus was stained as blue. Leading edge morphology of 3T3 fibroblasts and 3T3 vim- cells were observed to be different inside the channel (Fig. 4). 3T3 fibroblast cells exhibit typical fan-like leading edge lamellipodia, which can be explained as the effect of vimentin on

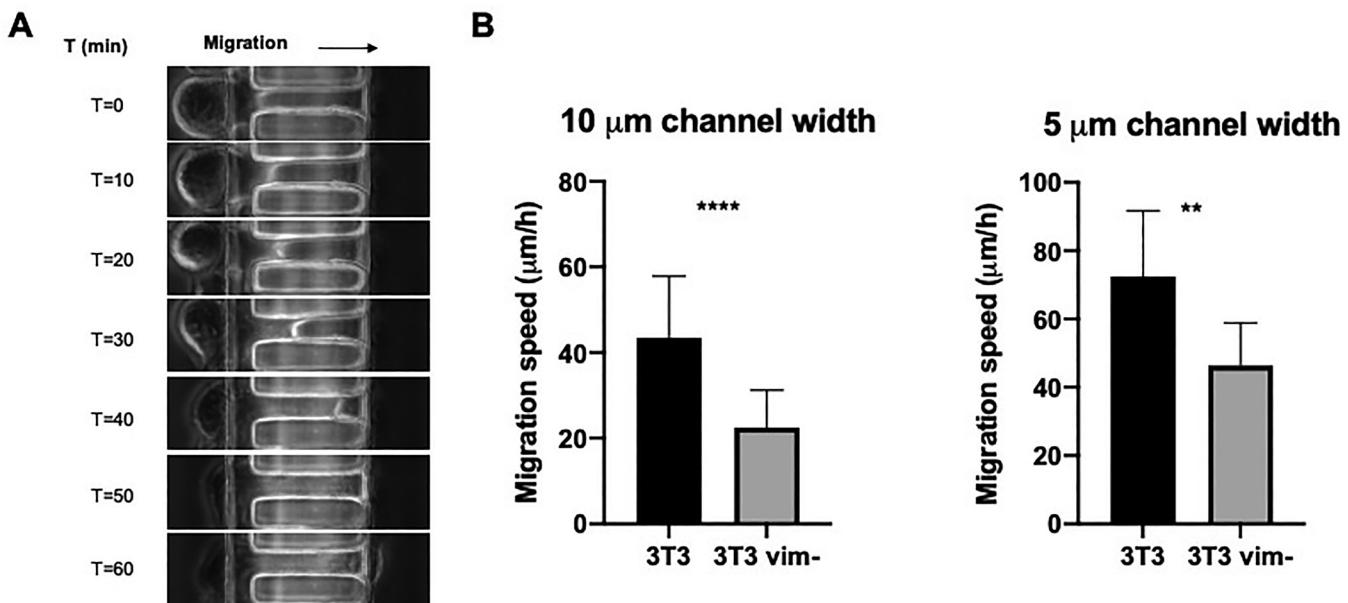


FIG. 3. (a) Phase-contrast time-lapse images of a cell moving through channel coated with collagen I. (b) Effect of vimentin on cell motility migration speed of 3T3 and 3T3 vim- cells in a channel. Effect of channel width migration speed of both cell line in 5 and 10 μm width channel (45–60 cells per condition, N = 3+ experiments). ***p < 0.0001; **p < 0.01.

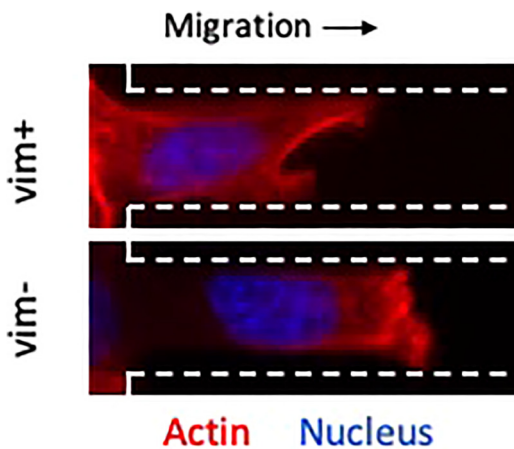


FIG. 4. Leading edge morphology inside microchannel of 3T3 cell and 3T3 vim- cells.

actin organization. 3T3 vim- cells project different leading edge structures, which are blunt-ended lobopodian protrusions. This means that 3T3 vim- cells are unable to establish the polarity required for motility, which could explain the inhibition of motility. Thus, the regulation of vimentin may act as a molecular signal that modulates the actin-based machinery responsible for moving cells.

CONCLUSIONS

In conclusion, a microfluidic device with collagen-coated 3D microchannels was fabricated to study the effect of vimentin on cell migration and leading edge protrusions. Cell passage rate through channels increased significantly after collagen coating of the microchannel, which provided a physiologically similar setting for this study. This device also revealed that interactions between the microchannel wall and cells inside microchannels are critical for cell 3D migration. Using this microchannel assay, vimentin knockdown cells showed lower cell motility characterized by lower migration speed inside microchannel, proving that vimentin can promote fibroblast cell directional migration in a 3D microenvironment. Moreover, 3T3 vim- cells showed blunt-ended lobopodian protrusions different from typical fan-like lamellipodia protrusions in 3T3 fibroblast cells. This distinction demonstrated that vimentin expression regulates actin cytoskeleton organization and affects cell motility.

SUPPLEMENTARY MATERIAL

See the [supplementary material](#) for movie of 3T3 and 3T3 vim- cell migration inside microchannel, figure of cell migration with marks of cell membrane, immunofluorescence imaging of cell leading edge morphology, confocal image of cell inside channel, and vimentin knockdown 3T3 western blotting analysis

AUTHORS' CONTRIBUTIONS

All authors contributed equally to this work.

ACKNOWLEDGMENTS

This work was supported by the National Science Foundation (NSF) (No. CBET-1805514).

DATA AVAILABILITY

The data that support the findings of this study are available within the article.

REFERENCES

- ¹J. Yang and R. A. Weinberg, *Dev. Cell* **14**(6), 818–829 (2008).
- ²R. Horwitz and D. Webb, *Curr. Biol.* **13**(19), R756–R759 (2003).
- ³G. P. Gupta and J. Massagué, *Cell* **127**(4), 679–695 (2006).
- ⁴P. Friedl and S. Alexander, *Cell* **147**(5), 992–1009 (2011).
- ⁵C. Frantz, K. M. Stewart, and V. M. Weaver, *J. Cell Sci.* **123**(Pt 24), 4195–4200 (2010).
- ⁶M. J. Bissell and D. Radisky, *Nat. Rev. Cancer* **1**(1), 46–54 (2001).
- ⁷D. Wirtz, K. Konstantopoulos, and P. C. Searson, *Nat. Rev. Cancer* **11**(7), 512–522 (2011).
- ⁸A. Berzat and A. Hall, *EMBO J.* **29**(16), 2734–2745 (2010).
- ⁹J. M. Muncie and V. M. Weaver, *Curr. Top. Dev. Biol.* **130**, 1–37 (2018).
- ¹⁰D. Hoffman-Kim, J. A. Mitchel, and R. V. Bellamkonda, *Annu. Rev. Biomed. Eng.* **12**, 203–231 (2010).
- ¹¹T. N. TruongVo, R. M. Kennedy, H. Chen, A. Chen, A. Berndt, M. Agarwal, L. Zhu, H. Nakshatri, J. Wallace, S. Na, H. Yokota, and J. E. Ryu, *J. Micromech. Microeng.* **27**(3), 035017 (2017).
- ¹²M. W. Tibbitt and K. S. Anseth, *Biotechnol. Bioeng.* **103**(4), 655–663 (2009).
- ¹³C. D. Paul, W.-C. Hung, D. Wirtz, and K. Konstantopoulos, *Annu. Rev. Biomed. Eng.* **18**(1), 159–180 (2016).
- ¹⁴T. Fujii, *Microelectron. Eng.* **61**–**62**, 907–914 (2002).
- ¹⁵N. Mor-Vaknin, A. Punturi, K. Sitwala, and D. M. Markovitz, *Nat. Cell Biol.* **5**(1), 59–63 (2003).
- ¹⁶A. Satelli and S. Li, *Cell. Mol. Life Sci.* **68**(18), 3033–3046 (2011).
- ¹⁷M. G. Mendez, S. I. Kojima, and R. D. Goldman, *FASEB J.* **24**(6), 1838–1851 (2010).
- ¹⁸B. Eckes, D. Dogic, E. Colucci-Guyon, N. Wang, A. Maniotis, D. Ingber, A. Merckling, F. Langa, M. Aumailley, A. Delouvee, V. Koteliansky, C. Babinet, and T. Krieg, *J. Cell Sci.* **111**(13), 1897–1907 (1998).
- ¹⁹B. Eckes, E. Colucci-Guyon, H. Smola, S. Nodder, C. Babinet, T. Krieg, and P. Martin, *J. Cell Sci.* **113**(13), 2455–2462 (2000).
- ²⁰B. T. Helfand, M. G. Mendez, S. N. P. Murthy, D. K. Shumaker, B. Grin, S. Mahammad, U. Aebi, T. Wedig, Y. I. Wu, K. M. Hahn, M. Inagaki, H. Herrmann, and R. D. Goldman, *Mol. Biol. Cell* **22**(8), 1274–1289 (2011).
- ²¹K. Vuoriluoto, H. Haugen, S. Kiviluoto, J. P. Mpindi, J. Nevo, C. Gjerdrum, C. Tiron, J. B. Lorens, and J. Ivaska, *Oncogene* **30**(12), 1436–1448 (2011).
- ²²R. J. Paccione, H. Miyazaki, V. Patel, A. Waseem, J. S. Gutkind, Z. E. Zehner, and W. A. Yeudall, *Mol. Cancer Ther.* **7**(9), 2894–2903 (2008).
- ²³M. G. Mendez, S.-I. Kojima, and R. D. Goldman, *FASEB J.* **24**(6), 1838–1851 (2010).
- ²⁴Y. Zhao, Q. Yan, X. Long, X. Chen, and Y. Wang, *Cell Biochem. Funct.* **26**(5), 571–577 (2008).
- ²⁵Y. Messica, A. Laser-Azogui, T. Volberg, Y. Elisha, K. Lysakovskaya, R. Eils, E. Gladilin, B. Geiger, and R. Beck, *Nano Lett.* **17**(11), 6941–6948 (2017).
- ²⁶E. Olaso, J.-P. Labrador, L. Wang, K. Ikeda, F. J. Eng, R. Klein, D. H. Lovett, H. C. Lin, and S. L. Friedman, *J. Biol. Chem.* **277**(5), 3606–3613 (2002).
- ²⁷W. Li, J. Fan, M. Chen, S. Guan, D. Sawcer, G. M. Bokoch, and D. T. Woodley, *Mol. Biol. Cell* **15**(1), 294–309 (2004).
- ²⁸R. Ananthakrishnan and A. Ehrlicher, *Int. J. Biol. Sci.* **3**(5), 303–317 (2007).
- ²⁹T. Svitkina, *Cold Spring Harbor Perspect. Biol.* **10**(1), a018267 (2018).
- ³⁰R. J. Petrie and K. M. Yamada, *J. Cell Sci.* **125**(24), 5917–5926 (2012).

- ³¹K. M. Yamada and M. Sixt, *Nat. Rev. Mol. Cell Biol.* **20**(12), 738–752 (2019).
- ³²W. Zhang, D. S. Choi, Y. H. Nguyen, J. Chang, and L. Qin, *Sci. Rep.* **3**(1), 2332 (2013).
- ³³M. Nishikawa, T. Yamamoto, N. Kojima, K. Kikuo, T. Fujii, and Y. Sakai, *Biotechnol. Bioeng.* **99**(6), 1472–1481 (2008).
- ³⁴C. Somaiah, A. Kumar, D. Mawrie, A. Sharma, S. D. Patil, J. Bhattacharyya, R. Swaminathan, and B. G. Jaganathan, *PLOS ONE* **10**(12), e0145068 (2015).
- ³⁵T. J. Herbst, J. B. McCarthy, E. C. Tsilibary, and L. T. Furcht, *The Journal of Cell Biology* **106**(4), 1365–1373 (1988).
- ³⁶J. Jacobelli, R. S. Friedman, M. A. Conti, A.-M. Lennon-Dumenil, M. Piel, C. M. Sorenson, R. S. Adelstein, and M. F. Krummel, *Nat. Immunol.* **11**(10), 953–961 (2010).
- ³⁷A. W. Holle, N. Govindan Kutty Devi, K. Clar, A. Fan, T. Saif, R. Kemkemer, and J. P. Spatz, *Nano Lett.* **19**(4), 2280–2290 (2019).
- ³⁸R. J. Petrie, N. Gavara, R. S. Chadwick, and K. M. Yamada, *J. Cell Biol.* **197**(3), 439–455 (2012).
- ³⁹B. Chen, G. Kumar, C. C. Co, and C.-C. Ho, *Sci. Rep.* **3**(1), 2827 (2013).
- ⁴⁰S. Munevar, Y. Wang, and M. Dembo, *Biophys. J.* **80**(4), 1744–1757 (2001).
- ⁴¹S. Munevar, Y.-I. Wang, and M. Dembo, *Mol. Biol. Cell* **12**(12), 3947–3954 (2001).
- ⁴²J. B. Bard and E. D. Hay, *J. Cell Biol.* **67**(2), 400–418 (1975).
- ⁴³J. T. Parsons, A. R. Horwitz, and M. A. Schwartz, *Nat. Rev. Mol. Cell Biol.* **11**(9), 633–643 (2010).
- ⁴⁴F. Grinnell and W. M. Petroll, *Annu. Rev. Cell Dev. Biol.* **26**(1), 335–361 (2010).